



Assessing the synergic effect of land use and climate change on the upper Betwa River catchment in Central India under present, past, and future climate scenarios

Amit Kumar¹ · Abhilash Singh¹ · Kumar Gaurav¹

Received: 2 August 2021 / Accepted: 22 February 2022
© The Author(s), under exclusive licence to Springer Nature B.V. 2022

Abstract

We use Soil and Water Assessment Tool (SWAT) to simulate the combined effects of land use/land cover (LU/LC) and climate change on the hydrological response of the Upper Betwa River Catchment (UBRC), a semi-arid region in Central India. We execute this model for two different time periods, 1982–2000 and 2001–2018, using the LU/LC data of 1990 and 2018, respectively. We classified the Landsat satellite images of 1990 and 2018 to obtain the dominant LU/LC classes (water body, built-up, forest, agriculture, and open land) in the catchment. The water body, built-up areas, and cropland have increased by 63%, 65%, and 3%, respectively, whereas forest cover and open land decreased by 16% and 23% in the UBRC from 1990 to 2018. The observed climate data in UBRC shows an increase in the average temperature and decrease in the total rainfall during the period between 1980 to 2018. Once the model is set up, we perform the calibration and validation by using the SWAT Calibration Uncertainty Program (SWAT-CUP). We considered two time periods (1991–1994 and 2001–2007) for the calibration and (1995–1998 and 2008–2014) for the validation. For both these time periods, the calibration and validation result of our model is satisfactory. The output of our calibrated model shows a relative decrease in rainfall (12%), surface runoff (21%), and percolation (9%) in the catchment during the period between 2001–2018 as compared to 1982–2000. Finally, we simulate the surface runoff and percolation in the UBRC using the future climate change scenario. We used the bias-corrected multi-model ensemble of CMIP6 GCMs for four different climate scenarios (2023–2100) by assuming no change in the existing LU/LC. We do this for two different time slices: one from 2023–2060 and the other from 2061–2100. For all the climate scenarios, rainfall and surface runoff in the catchment are expected to decrease by 15–40% and 50–79% as compared to the baseline period of 1982–2018. Percolation in the catchment will have a mixed response. It is expected to decrease by 18% in the middle part of the catchment and increase about 25% in the remaining parts of the catchment.

Keywords Climate change · CMIP6 · ERA5 · Land use and land cover change · SWAT · Semi-arid catchment

✉ Amit Kumar
amit17@iiserb.ac.in

Extended author information available on the last page of the article

1 Introduction

Arid and semi-arid regions are highly sensitive to human alterations of the earth system and climate change (Huang et al. 2016). Approximately 15% of the world population resides in these regions and primarily depends on rainfall to meet their water demand for agriculture, industrial, and domestic purposes (Liu and Xia 2004; Schwinning et al. 2004). According to Huang et al. (2016), worldwide the total area of semi-arid region has increased by 7% during 1990–2004. It is expected that the climate change together with the LU/LC change beyond a critical level can lead to food and water scarcity in the dryland regions (Abbas et al. 2021b; Abbas and Dastgeer 2021). World is currently facing an alarming rate of increase in the CO₂ concentration. This has resulted in the mean temperature to increase by 1°C from the beginning of the industrial revolution (Li et al. 2020). The global warming is projected to increase further. In this changing climate, the frequency of drought events is likely to increase (Abbas and Dastgeer 2021; Aadhar and Mishra 2020). It will put immense stress on the vegetation cover, water resources, and agricultural productivity, particularly in the dry land regions (Abbas et al. 2020, 2021a; Yaseen et al. 2020).

About 45% of India's landmass is characterized by an arid and semi-arid climate that supports nearly 35% of its population and livestock. The sustenance of water resources in these regions depends on the Indian summer monsoon rainfall which contributes nearly 80% of freshwater resources. In the recent decades, Central India has witnessed a noticeable changes in the climate and LU/LC. Such changes have been attributed as the leading factors for the weakening of summer monsoon rainfall (Paul et al. 2016). The mean annual temperature (1960–2017) in Central India has increased by 0.05°C per decade and the precipitation (1950–2015) has decreased by about 10–20% (Roxy et al. 2017; Shah and Srivastava 2019). As a consequence, the frequency of drought has increased by 50% in the past two decades (Saharwardi et al. 2021). The groundwater table has declined in the regions where monsoon rainfall has decreased (Asoka et al. 2017). The extreme rainfall events have increased by 10–30% and are projected to increase further (Rao et al. 2014; Sharmila et al. 2015; Roxy et al. 2017). These factors together have severely impacted the regional water availability. It is thus important to study the combined impact of climate and LU/LC changes on the hydrological processes for better management of water resources in the semi-arid river catchments (Babar and Ramesh 2015; Wang et al. 2006; Chawla and Mujumdar 2015; Chanapathi and Thatikonda 2020; Kundu et al. 2017a; Wagner et al. 2016; Hengade and Eldho 2016).

Several studies have been conducted to evaluate the combined impact of climate and LU/LC on the hydrological processes of different river basins in India (Chawla and Mujumdar 2015; Kundu et al. 2017a; Chanapathi and Thatikonda 2020; Wagner et al. 2016). For example, Tsarouchi and Buytaert (2018) studied the effect of LU/LC and climate change on the Ganga basin. They observed that the combined effect of LU/LC and climate change has a high impact on the hydrological cycle of the upper Ganga River basin as compared to the scenario considering the climate change alone. Sinha et al. (2020) observed that the climate has a larger (70–90%) impact than LU/LC on surface runoff and sediment yield in the Valapattanam River basin in South India. Narsimlu et al. (2013) investigated the impact of future climate change in the upper Sind River basin, India, using the Providing REgional Climates for Impacts Studies (PRECIS) climate and SWAT model. They reported streamflow is likely to increase by 16% and 93% by the middle and end of the twenty-first century, respectively. Swain et al. (2020) observed that climate change has influenced the streamflow variability more than the LU/LC changes in the Brahmani-Baitarani River basin,

India. Chanapathi and Thatikonda (2020) projected the synergic effect of climate and LU/LC change by using the SWAT model. They observed by the end of the twenty-first century, the surface runoff, streamflow, and water yield will increase by 50% under the RCP 4.5 scenario in the Krishna River basin, India. Kundu et al. (2017b) reported that the runoff in the Narmada River in Central India has increased in response to LU/LC change in the catchment. Hengade and Eldho (2016) noticed that the decrease in rainfall by 1.7% has resulted in a reduction in surface runoff (7.8%) in the Godavari River basin, India. Desai et al. (2020) evaluated the projected impact of climate change under CMIP5 scenario in the Betwa River basin. They observed that the surface runoff is expected to increase by 4–29% and 12–48% during 2040–2069 and 2070–2099, respectively. To our knowledge, such studies have not been conducted to assess the synergic effect of climate and LU/LC in the upper Betwa River catchment. According to a study by Gosain et al. (2006), many river basins of India will face freshwater scarcity. The Betwa River is considered a lifeline of Madhya Pradesh. The Betwa River basin has experienced several changes in the past few decades, such as weakening of summer monsoon rainfall, enhanced frequency of extreme rainfall events, and LU/LC changes simultaneously (Paul et al. 2016; Roxy et al. 2017; Palmate 2017). It is therefore important to assess the combined effect of climate and LU/LC in the catchment under the past, present, and projected climate change scenarios.

Hydrological and climate models play an important role to quantify the impact of these factors on different hydrological components. The selection of hydrological models is user dependent and relies on data availability, site-specific problems, cost involvement, and the accuracy of the models (Mendoza et al. 2015). In addition, different regional or global climate models such as the Coordinated Regional Downscaling Experiment (CORDEX), PRECIS, Regional Climate Model system (RegCM), and Coupled Model Intercomparison Project (CMIP) 1–6 are used to estimate the future hydrological budget. This study evaluates the combined impact of climate and LU/LC change on the surface runoff and percolation in the UBRC. We used SWAT, a semi-distributed hydrological model with historical (1980–2018) and projected (2023–2100) climate data, to simulate the hydrological processes of the UBRC. We assess the surface runoff and percolation under four different climate scenarios using bias-corrected multi-model ensembles of Coupled Model Intercomparison Project (CMIP6) datasets. The outcome of this study can be useful in policy-making and strategic planning, especially in agriculture and water resource management in semi-arid catchments.

2 Study area

The UBRC is a part of the Betwa River, a tributary of the Yamuna River. It lies between latitudes 22°52'5''N to 24°54'5''N and longitudes 77°5'45''E to 78°09'31''E in the Central India. Total area of the catchment is about 9322 km², and the total length of Betwa River within UBRC is about 127 km. The Betwa River originates from Barkhera Village in the Vindhyan Ranges of Raisen District, Madhya Pradesh, and flows towards the northeast direction. The major tributaries in the UBRC are Baen, Sagar, and Halali rivers (Fig. 1). The Betwa River flows through different lithology, i.e., basalt, sandstone, shale, alluvial soil, and sand (Fig. 1). The average elevation in UBRC ranges between 370 and 669 m. The major soil types in the catchment are loamy, sandy, and clay. The annual average discharge of the UBRC at Kurwai gauging site is 200 m³/s. It receives maximum flow (90%) during the southwest summer monsoon (Fig. 2). The entire UBR catchment falls in the semi-arid

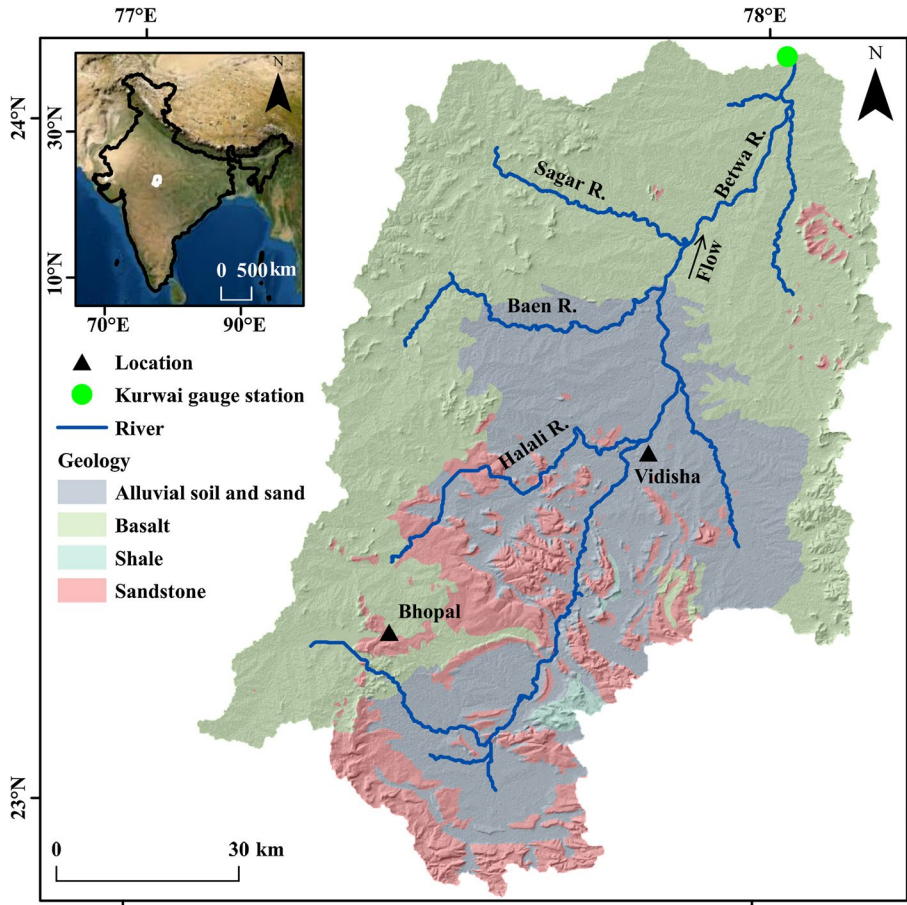


Fig. 1 Location of the Upper Betwa River catchment in Central India (©Google Earth). Lines in blue are the major stream network in the catchment, circle in blue at the outlet is the gauge station. Regions shown in different colors represent the geology of the catchment

climatic region. The annual average precipitation in the catchment is about 1153 mm, having the maximum and minimum temperature of 40°C and 2°C, respectively. About 90% of the total precipitation occurs during the monsoon period from June to September. The groundwater level (GWL) during pre- and post-monsoon varies between 2.6 and 16.4 and between 1.2 and 9.4 below groundwater level in meter (bglm), respectively (Naik et al. 2021). The dominant LU/LC in UBRC is water body (0.7%), agricultural land (80%), built-up (2%), open land (1%), and forest cover (15%).

3 Data and methodology

We used observed and simulated climate model products, river discharge (gauge station), satellite images, and other physical data (topography and soil types). Table 1 reports the detailed description of the data. Our climate data archive consists of rainfall,

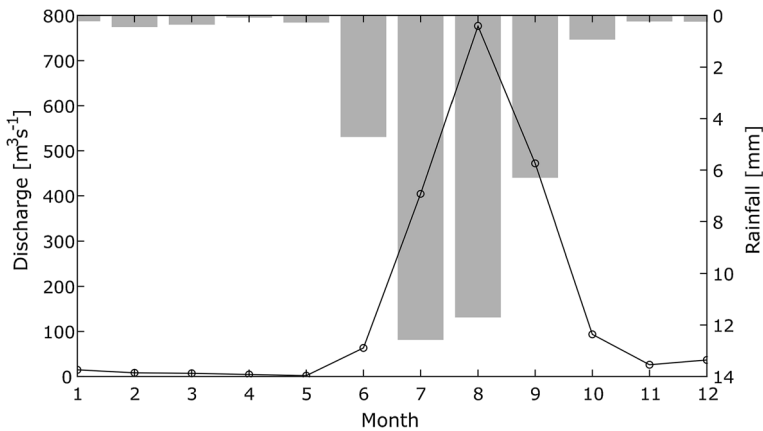


Fig. 2 Monthly average discharge and rainfall plotted for a period between 1991–2008. Line in the graph represents the streamflow, and bars illustrate the rainfall

Table 1 Details of the climate, physical, and gauge data used in this study

Data type	Parameter	Source	Time	Resolution
Climate data—historical	Rainfall	IMD	1980–2018	0.25°
	Temperature	IMD	1980–2018	1 (0.25°)*
	Wind speed	ERA 5	1980–2018	0.25°
	Solar radiation	ERA 5	1980–2018	0.25°
	Relative humidity	ERA 5	1980–2018	0.25°
Climate data—future	Rainfall	MIROC6 IPSL-CM6A-LR NorESM	1980–2100	
	Temperature	MIROC6 IPSL-CM6A-LR NorESM2-MM	1980–2100	
Physical data	Soil data	FAO		1 km
	Land use	Landsat5,8	1990, 2018	30 m
	Topography	SRTM		90 m
Gauge data	River discharge	MPWRD	1991–2014	Daily

*Resampled at (0.25°) resolution

temperature, relative humidity, wind speed, and solar radiation. We obtained the daily rainfall and temperature (minimum and maximum) for a period between 1980–2018 at a grid resolution of $0.25^\circ \times 0.25^\circ$ and $1^\circ \times 1^\circ$, respectively, from the Indian Meteorological Department (IMD) (<https://www.imdpune.gov.in>). For the same time period, we have downloaded the relative humidity, wind speed, and solar radiation reanalysis product from ERA5 of the European Centre for Medium-Range Weather Forecasting (ECMWF) (<https://cds.climate.copernicus.eu>) at a grid resolution $0.25^\circ \times 0.25^\circ$. We obtained the simulated rainfall and temperature from CMIP6 Global Climate Models (GCMs) such as MIROC 6, NorESM2-MM, and IPSL-CM6A-LR for a period from 1980 to 2100. We acquired daily discharge of the Betwa River at Kurwai gauge station for a period

between 1991–2014 from Madhya Pradesh Water Resource Department (MPWRD). We downloaded the soil map of the Upper Betwa River catchment at 1 km spatial resolution from the official Website of waterbase (<http://www.waterbase.org/>). We obtained Landsat 5 and Landsat 8 satellite images for February 16, 1990, and March 17, 2018, respectively, from the official Website of USGS (<https://earthexplorer.usgs.gov/>). To keep the same seasonality, we ensured the closest date when acquiring the images of different years. We have also downloaded the digital elevation model (DEM) at 90 m spatial resolution from Shuttle Radar Topographic Mission (SRTM) (<http://www.cgiar-csi.org/data/srtm-90m-digital-elevation-database-v4-1>).

3.1 Data processing

3.1.1 Climate data

Except for the temperature and the GCMs, spatial resolution of all the climate data is 0.25° . To have a similar resolution, we resampled them to a common grid size 0.25° by using bilinear interpolation (Vu et al. 2012; Aadhar and Mishra 2020). We then performed trend analysis of the observed climate data. We identify the magnitude of the trend using Sen's slope method (Devi et al. 2020) and conducted Mann–Kendall trend test (Mann 1945). It is a nonparametric test that is used to determine the monotonically increasing and decreasing trends or abrupt changes depicted by its three alternate hypotheses: positive, negative, and no trend. It has a broader application in meteorology and hydrology (Ahn and Merwade 2014; Kumar et al. 2021).

To assess the impact of climate change on the hydrological processes, we need projected climate variables. We have used the rainfall and temperature projection from CMIP6 for a period from 2023 to 2100. CMIP6 consists of several earth system models (Eyring et al. 2016). This is an updated version of CMIP in terms of the fine spatial resolutions, improved cloud microphysical mechanisms, and addition of earth system components such as biogeochemical cycles and ice sheets. Also, the future CMIP6 scenario is more advanced than the previous versions. It uses the socioeconomic pathways along with CMIP5 scenarios that allow more realistic future projections (Eyring et al. 2019). We selected MIROC6, IPSL-CM6A-LR, and NorESM2-MM, as they are best suited for the South-Asian regions (Aadhar and Mishra 2020). Due to their coarser resolution, GCMs are not able to capture the regional phenomenon realistically (Chawla and Mujumdar 2015).

Further, these models are vulnerable due to systematic errors associated with the forcing climate models and scenarios. The bias correction largely minimizes these errors. There are various methods for bias correction of the rainfall and temperature data, such as distribution mapping, linear scaling, variance scaling, and delta change approach. The distribution mapping-based bias correction is capable of removing the bias present in the projected data effectively. We applied the cumulative distribution function (CDF) matching for bias correction from the projected data (rainfall and temperature) by taking the observed values as a reference before feeding them into the hydrological model (Reichle and Koster 2004; Singh et al. 2020; Zhang et al. 2018; Teutschbein and Seibert 2012; Luo et al. 2018). It transfers the CDFs of projected data based on past observations. The Taylor diagrams (Fig. 3) illustrate the post-bias correction statistics of GCMs and observed variables for the period of 1980–2014. It is a two-dimensional graphical representation to visualize the similarity of GCMs with respect to the observed data sets, which is quantified based on the correlation coefficient, root-mean-square error, and standard deviation (Taylor 2001). We observed that

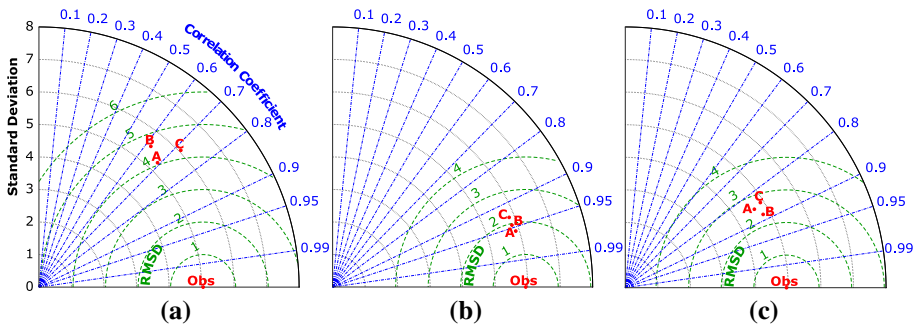


Fig. 3 Taylor diagram **a** rainfall (mm), **b** T_{max} ($^{\circ}C$) and **c** T_{min} ($^{\circ}C$) of CMIP6 GCMs (A:MIROC6 B:NorESM2-MM C:IPSL-CM6A-LR) with reference to IMD(Obs) for the period of 1980–2014

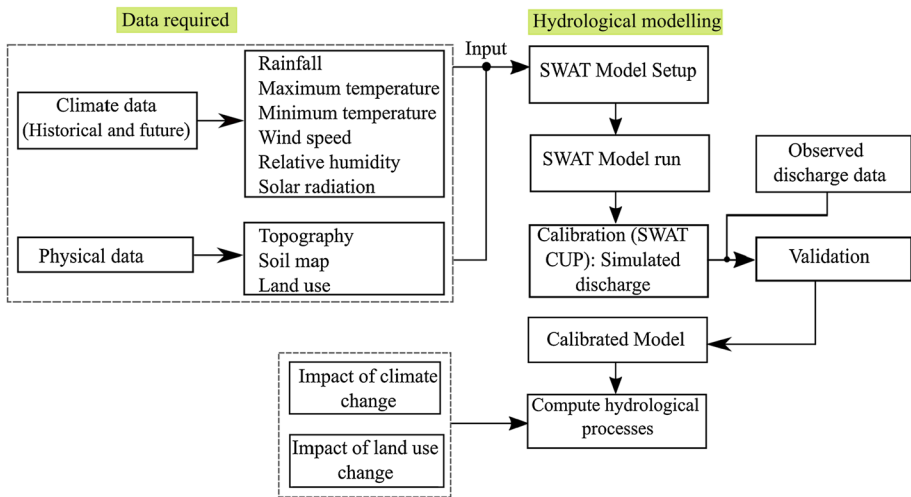


Fig. 4 Flowchart adopted in this study

the maximum temperature (T_{max}) and minimum temperature (T_{min}) for all three models are clustered together and closer to the observed temperature (Fig. 3). As far as rainfall is concerned, all the models slightly deviate from observation. We used the ensemble of all models for the future projection of hydrological processes.

Further, pathways explaining how the anthropogenic drivers such as GHGs and aerosols will be consistent with the future socioeconomic developments are known as the climate change scenario. It plays an important role in understanding and assessing climate change and its impact on improving adaptation and mitigation strategies. We have used different shared socioeconomic pathways (SSPs), SSP126, SSP245, SSP370, and SSP585, which is an updated version of previous representative concentration pathways (RCPs) in CMIP5 (O’Neill et al. 2016; Wang et al. 2018; Gupta et al. 2020). The prefix of SSPs is represented as a-b, where **a** indicates the specific SSP and **b** represents the radiative forcing level such as 1.6, 4.5, 7.0, and 8.5 w/m^2 . Table 2 represents the different features of SSP scenarios.

Table 2 Descriptions of different SSPs (adopted from O'Neill et al. 2014)

SSPs	Challenges	Salient features
SSP1	Mitigation and adaption is low	Rapid sustainable development with technological advancement in an eco-friendly way using less carbon energy and highly productive land.
SSP2	Moderate mitigation and adaption	Transition phase of SSP1 and SSP3.
SSP3	High mitigation and adaption	Moderate economic growth and rapid population growth, delayed technological advancements, low adaptive capacity.
SSP5	High mitigation and low adaption	Relatively faster economic development, enhanced energy requirement, less investment in non-conventional energy sources and low population growth, less with more equitable resource distributions, vulnerable to climate change and a better world for adaptation.

3.1.2 Land use and land cover classification

We used green, red, and near-infrared (NIR) bands of Landsat 5 and 8 images for LU/LC classification. We applied the maximum likelihood algorithm to classify the image pixels into five different LU/LC classes (i.e., water body, forest, cropland, open land, and built-up). We then assessed the accuracy of the classified images by using the overall accuracy and Kappa statistics. In doing so, we generated 400 random points for all the LU/LC classes on the referenced (Google Earth) map. The overall and Kappa statistics for land use of 1990 are 0.91% and 0.86, and for the year 2018 are 0.92% and 0.89. The accuracy of image classification result is satisfactory.

3.2 SWAT Model setup

We set up SWAT model to simulate hydrological responses of the UBRC. This is a semi-distributed model that partitions the catchment into different sub-watersheds and further into several hydrological response units (HRUs) on the basis of similar soil types, LU/LC, and slope. SWAT model uses Soil Conservation Services (SCS) curve number method to compute the surface runoff (Anand et al. 2018). Finally, this model solves the water budget equation (Eq. 1) to compute the different components of the hydrological cycle according to;

$$SW_t = SW_0 + \sum_{i=1}^t (R_{day} - Q_{surf} - E_a - W_{seep} - Q_{gw}) \quad (1)$$

where, SW_t is the soil water content after time step t on the day i (mm), SW_0 is the initial soil and water content on the day i (mm), R_{day} is the amount of precipitation on the day i (mm), Q_{surf} is the amount of surface runoff on the day i (mm), E_a is the amount of evapotranspiration on day i (mm), W_{seep} is the amount of water entering the vadose zone from the soil profile on day i (mm), and Q_{gw} is the amount of return flow as drainage to the surface water on the day i (mm).

SWAT requires various input parameters such as rainfall, temperature (minimum, maximum), relative humidity, wind speed, solar radiation, elevation, soil, and LU/LC. We set up the model for two different time periods from 1980–2000 and from 1998–2018. Figure 4 shows the detailed procedure of model setup. We used LU/LC map for years 1990 and 2018 as a baseline for the simulation of 1980–2000 and 1998–2018, respectively. We used the initial two years 1980–1982 and 1998–2000 for both the simulations as a warm-up period. We then execute the model to simulate surface runoff and percolation into the ground in response to a given rainfall event. The model provides various other outputs such as evapotranspiration, water yield, and river discharge. We use in-situ discharge measured at the gauge station to calibrate and validate the model using SWAT-CUP module. The first step of calibration is sensitivity analysis. It is done using a global method (Arnold et al. 2012) in which all the input model parameters are allowed to change. Hereafter, the calibration is performed using model-sensitive parameters by comparing the observed and simulated flow. Further, the validation is carried out by changing the different time periods of observed and simulated flow, and subsequently a calibrated model is used for simulation of different hydrological processes of UBRC.

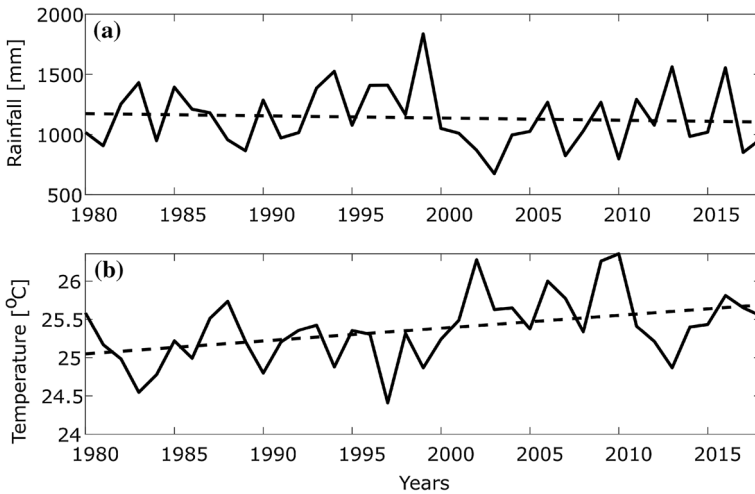


Fig. 5 Observed annual average trend of **a** rainfall and **b** temperature during 1980–2018. (Trend based on p value < 0.05 at 95% confidence level in Mann–Kendall test)

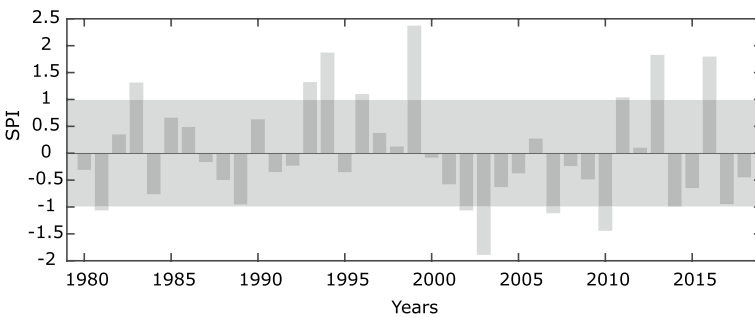


Fig. 6 Standardized precipitation Index (SPI) for the monsoon season during 1980–2018. Shaded region (SPI -0.99 to 0.99) shows the normal precipitation condition. SPI in range $(-1 \leq -2)$ and $(1 \leq 2)$ suggests drought and wet condition

Finally, we evaluate the performance of model using different statistical matrices such as coefficient of determination R^2 , Nash–Sutcliffe efficiency (NSE), percent bias (PBIAS), and ratio of root-mean-square error to measured standard deviation (RSR) (Moriassi et al. 2007).

4 Results

4.1 Observed climate in the catchment

Figure 5a shows the annual rainfall trend from 1980 to 2018 in the study area. The total precipitation has decreased by 1.8 mm, though it is not statistically significant (Fig. 5a). UBRC receives about 90% of the total rainfall during the Indian summer monsoon (JJAS).

The monsoon rainfall from 1980 to 2018 exhibits a declining trend. We calculated the SPI to characterize the monsoon rainfall (Fig. 6). According to SPI values, they can be categorized as wet (1–2), normal (–0.99 to 0.99), and drought (–1 to –2) events (Hayes et al. 1999; Abbas and Kousar 2021). We observed that during 1980–2000 one drought (1981) and five wet (1983, 1993, 1994, 1996, and 1999) events have occurred, whereas, during 2000–2018, four droughts (2002, 2003, 2007, and 2010) and three wet (2011, 2013, and 2016) events have occurred. This indicates that the frequency of drought events has increased in the UBRC after 2000. We have also performed the trend analysis for annual mean temperature, relative humidity, solar radiation, and wind speed. We observed a significant increase in the annual mean temperature (0.01°C), relative humidity (0.13%), and a decrease in the wind speed (0.39 m/s) and solar radiation (0.30 watt/m²) during 1980–2018 (Fig. 5b).

4.2 Land use and land cover change

Figure 7 shows the LU and LC maps of the UBRC. The dominant land cover in UBRC is cropland followed by forest, built-up, open land, and water body. We observed that the water body, built-up, and cropland in 2018 have increased by 63, 65, and 3%, respectively, as compared to 1990 (Fig. 7). During the same period, forest and open land areas have decreased by 16 and 23%. An increase in the water bodies is primarily because of the construction of two small reservoirs in the catchment after 2011. The increasing population has probably resulted in the increase in built-up, cropland, and decline in the forest and

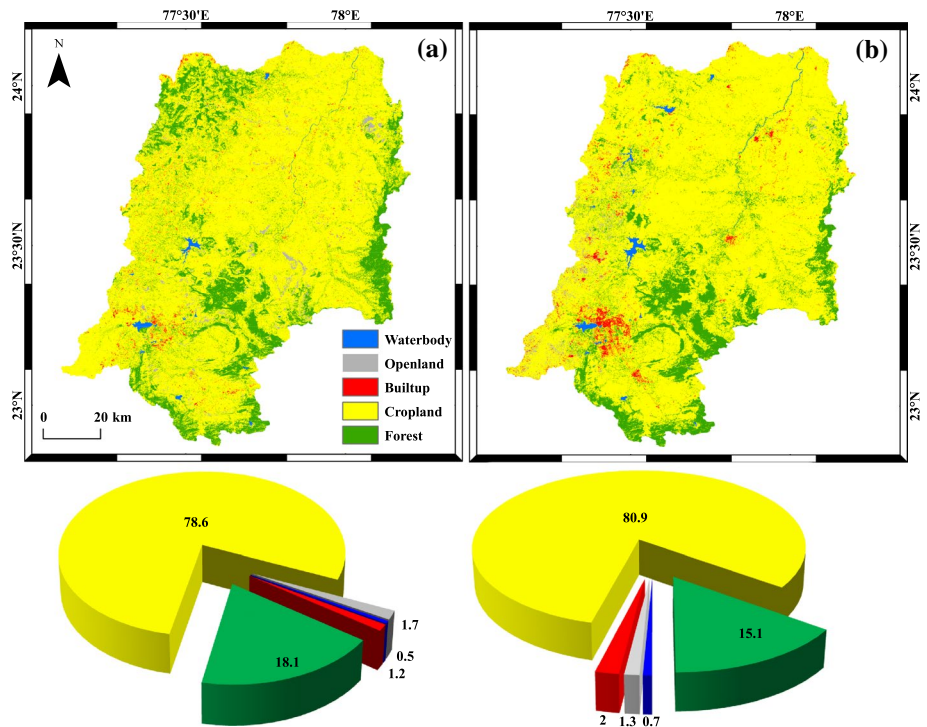


Fig. 7 Land use/land cover change maps of the Upper Betwa River catchment **a** 1990 **b** 2018. Pie charts show the area of respective LU/LC classes in percentage

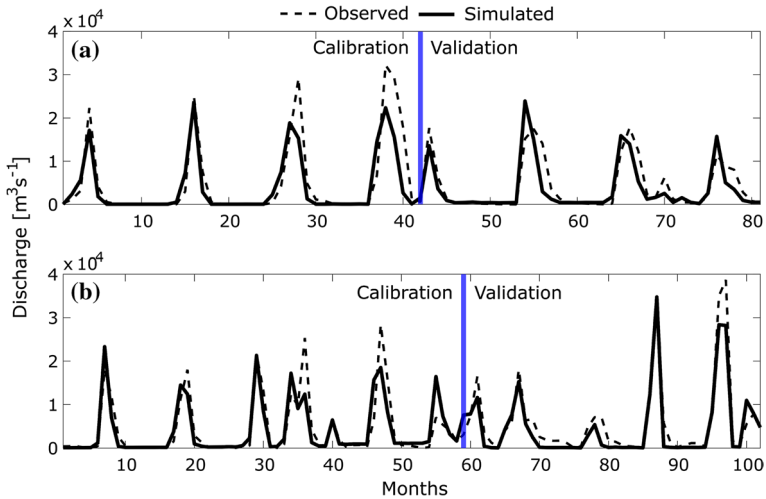


Fig. 8 Monthly time series plot of observed and simulated flow of UBRC during the calibration **a** 1991–1994 **b** 2001–2007, and validation **a** 1995–1998 **b** 2008–2014 periods of the SWAT Model

Table 3 Statistical performance evaluation of the model calibration and validation report

	R^2	NSE	PBIAS	RSR	Performance
Calibration (1991–1994)	0.7	0.69	21.9	0.56	Satisfactory
Validation (1995–1998)	0.67	0.66	13.6	0.59	Satisfactory
Calibration (2001–2007)	0.63	0.63	5.3	0.61	Satisfactory
Validation (2008–2014)	0.74	0.73	20.1	0.52	Satisfactory

open land. According to Palmate (2017), by 2100 the water bodies and agricultural land are expected to decrease by about 0.71% and 6.41%, respectively, whereas forest and barren land are expected to increase by 4%.

4.3 Model calibration, validation, and sensitivity analysis

Calibration, validation, and sensitivity analysis of the SWAT model are done for both the simulations in SWAT-CUP using Sequential Uncertainty Fitting version 2 (SUFI-2) (Dubey et al. 2020). We first performed the model calibration for 1991–1994 and 2001–2007. We then performed validation of model simulations for the periods 1995–1998 and 2008–2014. Table 3 reports the performance metrics of the calibration and validation. The model performance for calibration and validation is satisfactory. Figure 8 shows the monthly time series of observed and simulated flow during calibration and validation. It indicates that our model can simulate both the low and high flow conditions with a small deviation. This is due to the fact that the SWAT model uses daily average rainfall instead of the intensity and duration of a storm event (Sinha et al. 2020).

Finally, we perform the sensitivity of the model. It suggests how sensitive is the model output in response to a given change in the magnitude of the input variables (Arnold et al. 2012). While calibrating the model for both simulation periods 1980–2000 and

Table 4 Sensitivity of different parameters of SWAT model during the simulation of 1982–2000 and 1998–2018

Parameters	Description	Min	Max	Rank (1982–2000)	Rank (2001–2018)
CH N2	Channel roughness coefficient	0	0.3	8	1
CH K2	Hydraulic conductivity of channel	0	200	2	2
ALPHA BF	Base flow alpha factor	0	1	1	3
OV N	Over land flow	0	30	4	4
EPCO	Plant evaporation compensation factor	0	1	13	5
SHALLST	Initial shallow aquifer depth	0	5000	15	6
RCHRG DP	Deep aquifer percolation fraction	0	1	19	7
MSK CO1	Coefficient to control the impact of storage time constant	0	10	11	8
SOL_K	Hydraulic conductivity of soil	0	500	10	9
FFCB	Field capacity water content	0	1	18	10
SOL_BD	Moist soil bulk density	0.9	2.5	3	11
GW DELAY	Groundwater delay	0	500	16	12
CN2	SCS runoff curve number for moisture condition II	35	90	9	13
GWQMN	Depth of shallow aquifer required for return flow	0	500	12	14
GW REVAP	Groundwater revap coefficient	0.02	0.2	6	15
SOL_AWC	Available water content	0	1	7	16
HRU SLP	Slope of hydrologic response unit	0	1	5	17
SURLAG	Surface runoff lag coefficient	0	25	14	18
ESCO	Soil evaporation compensation factor	0	1	17	19

1998–2018, we considered 19 different sensitive parameters (Table 4). We keep the upper and lower bound of the parameters constant for both the simulations. During the simulation period 1980–2000, we observed that the most sensitive parameters to the streamflow are alpha base flow (ALPHA_BF), hydraulic conductivity of the channel (CH_K2), and soil bulk density (SOL_BD), whereas for the simulation period 1998–2018, the most sensitive parameters are the Manning coefficient of the channel (CH_N2), hydraulic conductivity of the channel (CH_K2), and alpha base flow (ALPHA_BF).

4.4 Hydrological response to LU/LC and climate change

To assess the hydrological response to LU/LC and climate change in the UBRC, we divided the whole basin into 25 sub-basins (Fig. 9). We then use the calibrated SWAT model to simulate the observed surface runoff and percolation. In doing so, We consider the observed data for two different time periods 1982–2000 and 2001–2018 to evaluate the impact of LU/LC and climate change. For a period during 1982–2000, the annual average rainfall varies in a range from 1017 to 1418 mm. This has reduced significantly to 915–1192 mm (about 12%) during 2001–2018 (Fig. 9a, b).

Rainfall and the physical characteristics of the catchment (e.g., soil, slope, LU/LC, and shape of the basin) play an important role in regulating the surface and subsurface hydrological processes such as runoff, percolation, and streamflow. We observed the annual

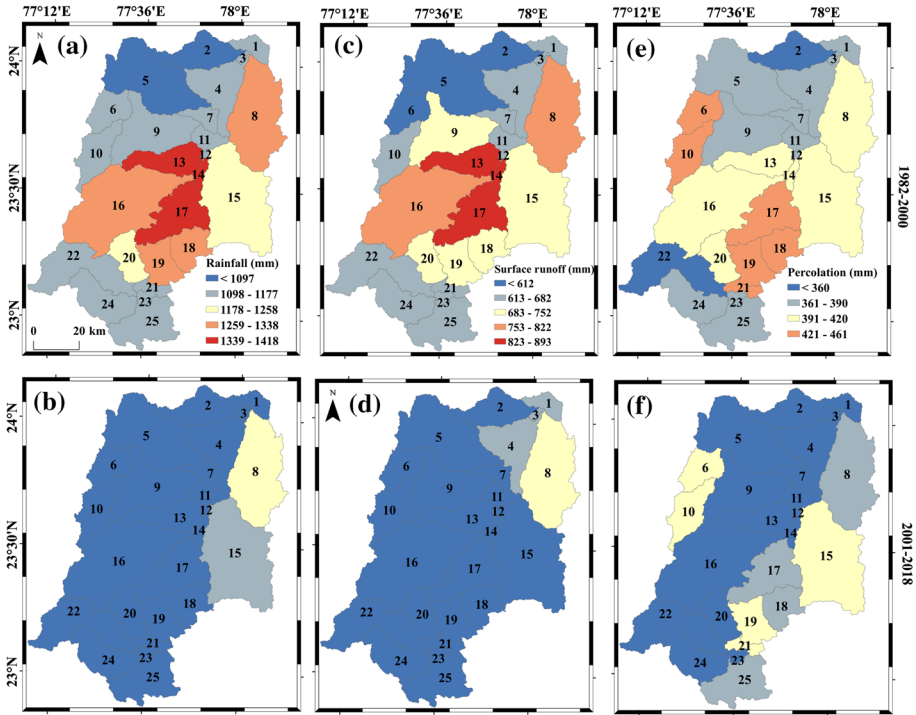


Fig. 9 Annual average observed changes (mm) in rainfall (a,b), surface runoff (c,d), and percolation (e,f) during time period of 1982–2000 (a, c, e) and 2001–2018 (b, d, f), respectively

average surface runoff has decreased by 21% in the entire basin during 2001–2018. Its annual average values vary between 542–893 mm during 1982–2000 and 459–687 mm during 2001–2018 (Fig. 9c, d).

Further, a similar response can be observed in percolation (Fig. 9e, f). It varies between 334–461 mm during 1982–2000 and from 320–400 mm during 2001–2018. It has decreased by 9% during 2001–2018. Apart from LU/LC and climate change, rapid irrigation and population growth might be responsible for reducing percolation.

Figure 9 shows the spatial variation in rainfall, surface runoff, and percolation. A large spatial variation in the rainfall over UBRC can be observed during the historical time period 1982–2000. We observed that sub-catchments 8, 13, 14, and 16–19 received the maximum rainfall (1259–1418 mm), whereas sub-catchments 2 and 5 received less than 1097 mm. In addition, during 2001–2018, UBRC received maximum rainfall (1098–1258 mm) in sub-catchments 8 and 15. The remaining sub-catchments have received less than 1097 mm rainfall. During 1982–2000, the surface runoff is largely distributed as per the spatial distribution of rainfall. We have also observed a larger spatial variability in percolation in the UBRC during 1982–2000.

4.5 Hydrology of the UBRC: future projections

To simulate the projected hydrological processes in the UBRC, we keep the LU/LC of 2018 constant and use the ensemble future rainfall and temperature. We considered the

other weather parameters as a baseline time period (1980–2018), as they do not have a significant influence on the regional hydrology (Dibaba and Demissie 1801). Further, we divide the future projection periods into two slices: the one from 2023–2060 and the other from 2061–2100. Rainfall in the catchment is expected to decrease in SSP126 and SSP245 by 21–40% and 24–42%, respectively, in the entire sub-basin during both the projected periods (Fig. 10). We observed that rainfall is expected to decrease relatively larger in the middle part of the UBRC. According to SSP370, it will decrease by 27–45% from 2023 to 2060 and 18–37% during 2061–2100. Further, according to SSP585, the rainfall is projected to decrease by 24–43% and 14–34%, respectively, during both periods.

In addition to rainfall, the surface runoff is expected to decrease by 50–79 % in all scenarios for both the projected time periods (Fig. 11). According to SSP126 and SSP245 scenarios, it is expected to decrease by 58–75% and 61–77%, respectively, during 2023–2060 in the entire UBRC; however, in the southern part of the basin, the magnitude will be relatively less (sub-basin 18–25). A similar trend exists in SSP370 and SSP585 climate scenarios. According to these scenarios, the surface runoff is projected to reduce by 64–79% during 2023–2060, while in the latter half, it is expected to decrease by 52–72% and 48–69%, respectively.

According to the scenarios discussed above, a weaker monsoon is expected during 2023–2060 as compared to the monsoon during the period from 2061–2100. This will eventually result in reduced rainfall (Fig. 10) and surface runoff (Fig. 11), which will ultimately lead to frequent drought events in the UBRC. The percolation is expected to have a mixed response (Fig. 12a–h). It is likely to decrease by 18% in the middle part and increase up to 25% in the southern and northern parts of the UBRC. In all the climatic scenarios, the percolation of rainfall into the ground will be comparatively less in the middle part of the UBRC during 2023–2060 than in 2061–2100.

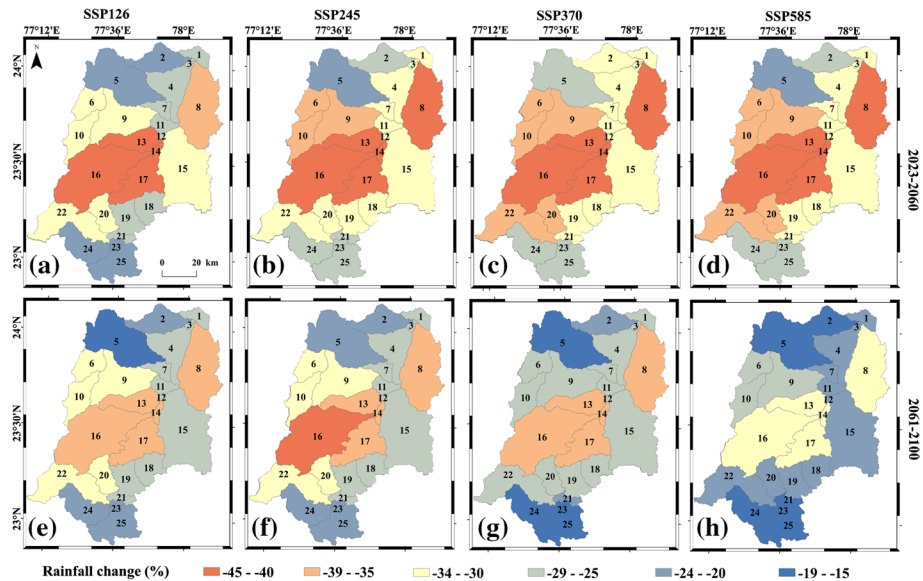


Fig. 10 Annual average future rainfall changes (%) during time period of 2023–2060 (a, b, c, d) and 2061–2100 (e, f, g, h) with reference to the base period 1982–2018. Figure (a, e) (b, f) (c, g), and (d, h) corresponds to SSP126, SSP245, SSP370, and SSP585 climate scenarios, respectively

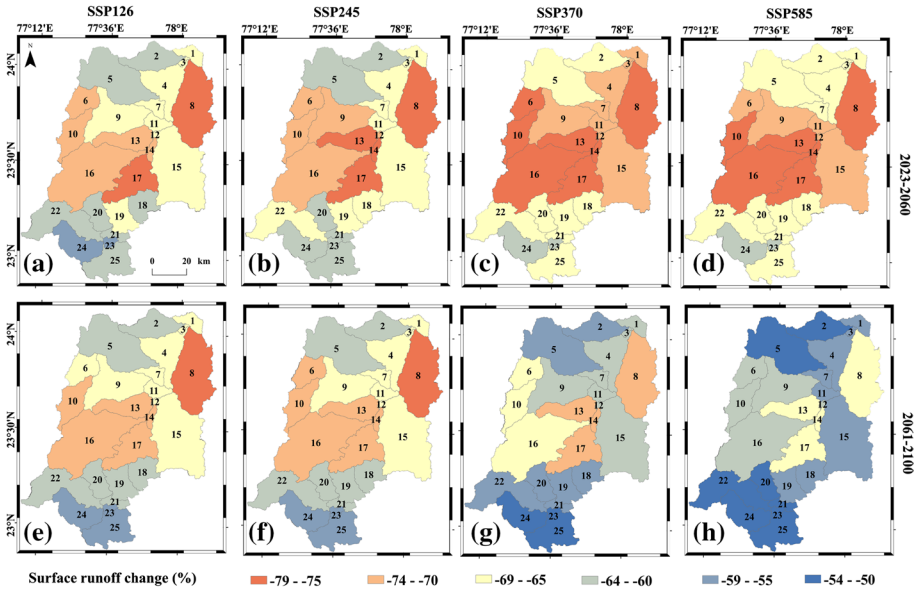


Fig. 11 Annual average future surface runoff changes (%) during time period of 2023–2060 (a, b, c, d) and 2061–2100 (e, f, g, h) with reference to the base period 1982–2018. Figure (a, e) (b, f) (c, g), and (d, h) corresponds to SSP126, SSP245, SSP370, and SSP585 climate scenarios, respectively

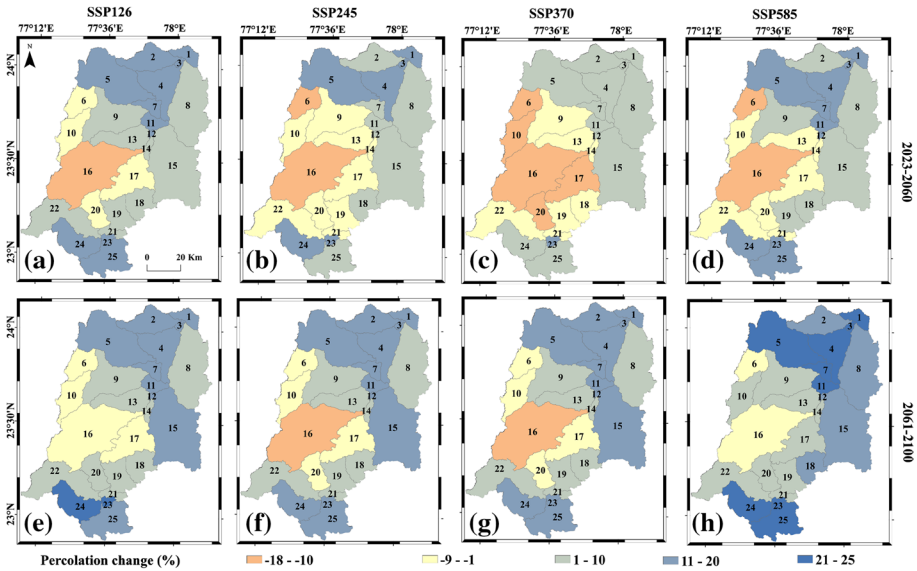


Fig. 12 Annual average future percolation changes (%) during time period of 2023–2060 (a, b, c, d) and 2061–2100 (e, f, g, h) with reference to the base period 1982–2018. Figure (a, e) (b, f) (c, g), and (d, h) corresponds to SSP126, SSP245, SSP370, and SSP585 climate scenarios, respectively

5 Discussion

We have investigated the combined effect of LU/LC and climate change on the surface runoff and percolation in the UBRC. To do this, we split the climate data into two time periods: 1982–2000 and 2001–2018. Since the LU/LC class changes gradually in the region, we used baseline LU/LC types for that time period to assess the synergic effect of climate change and LU/LC in the hydrology of the UBRC.

We observed a decrease in the annual average surface runoff (21%) and percolation (9%) in the catchment during the period between 2001–2018. We noticed that the change in surface runoff is comparable to the pattern of rainfall change in most of the sub-catchments. Chawla and Mujumdar (2015) found that the climate has more influence than the LU/LC change on the surface runoff. For instance, land use such as built-up and water body have changed mainly in sub-catchment number 16. The total annual average rainfall during 1982–2000 was about 1337 mm, which has decreased to 1014 mm during 2001–2018. This difference in rainfall has reduced the surface runoff by 159 mm.

We observed that the percolation in the sub-catchment 16 has decreased by 68 mm during 2001–2018 as compared to 1982–2000. This result compares with the other similar studies conducted on the semi-arid catchment in India. For example, Tanksali and Soraganvi (2021) observed that due to the effect of LU/LC change the surface runoff in the Krishna River basin has reduced by 29%. During the simulation period 2001–2018, we have only changed the LU/LC and weather parameters, and other variables such as soil and slope remain unchanged. This suggests that the LU/LC and climate change have resulted in the reduction in surface runoff and percolation in the UBRC.

We further evaluate the potential causes of reduced runoff and percolation other than the LU/LC and climate change. In doing so, we calculated the SPI for the monsoon season to characterize the dry and wet events. We then select the corresponding year to identify the relationship between surface runoff and percolation in the catchment. We observed during 1980–2018, the largest wet and dry events occurred in 1999 and 2003 (Fig. 6). We noticed that in the wet year of 1999, the runoff has increased by 6%, and the percolation has decreased by 2%. In the dry year 2003, the surface runoff has decreased by 8%, and percolation has increased by 6%. Here, it is important to notice that apart from the LU/LC and initial boundary condition of the catchment, the rainfall pattern largely controls the surface runoff. However, in the case of percolation, it depends on the retention time of water on the surface. Any increase or decrease in percolation may also be due to the availability of soil moisture and pre-monsoon rainfall in a given year.

We observed that for all the future climate scenarios, surface runoff and percolation are expected to decrease in the catchment. This can be attributed to the increased frequency of dry events in the future (Fig. 13). A study conducted by Desai et al. (2020) in the Betwa River basin found that the rainfall and surface runoff will increase in the future. This is in contrast to our result. We guess this discrepancy is possibly due to the use of different future climate models and base time periods. Desai et al. (2020) have considered a single model (MIROC5) of CMIP5 for the base period (1960–1990).

The UBRC receives maximum rainfall (about 90%) during the Indian summer monsoon. Most of the surface runoff (about 95%) occurred during this period. We observed that the surface runoff in the catchment has decreased by 18% during the monsoon season of 2001–2018 as compared to 1982–2000. It is therefore crucial to conserve the surface water in the UBRC to ensure sustainable water management to cope up with the projected LU/LC and climate change. The irrigation facilities should be upgraded to improve

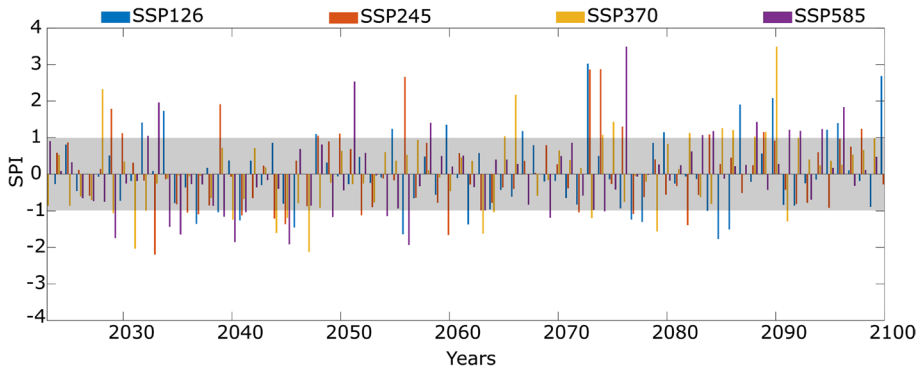


Fig. 13 SPI for the monsoon season according to the future climate projections of SSP126, SSP245, SSP370, and SSP585 for the period between 2023 and 2100. Shaded region (SPI -0.99 to 0.99) shows the normal precipitation condition. SPI values (-1 to -2) and (1 – 2) suggest drought and wet condition

agricultural productivity throughout the year. In addition, the storage of rainfall during the monsoon season by using appropriate methods such as rainwater harvesting and artificial recharge facilities should be adopted for proper water supply during non-monsoon months in the catchment. This study can be useful for policymakers to make well-informed law and adaptive strategies to mitigate risk associated with climate changes under the different future climate scenarios of the catchment.

6 Conclusions

We used the SWAT model to assess the impact of LU/LC and climate change on the hydrological response of the Upper Betwa River catchment in Central India. We have executed this model for two different times 1982–2000 and 2001–2018 by considering the LU/LC data of 1990 and 2018, respectively. The model output shows a decrease in the rainfall (12%), surface runoff (21%), and percolation (9%) in the UBRC during the period between 2001–2018 as compared to 1982–2000.

Considering the future climate change projection scenarios (SSP126, SSP245, SSP370, and SSP585) from 2023–2100 and assuming no change in the LU/LC in the catchment suggest a significant impact on the rainfall, surface runoff, and percolation from the baseline period 1982–2018. In all these climate scenarios, rainfall (15–40%) and surface runoff (50–79%) are expected to decrease, whereas the percolation will have a mixed response. The percolation is likely to decrease (18%) in the middle part of the catchment and increase (25%) in the remaining areas. This decline in the rainfall, surface runoff, and percolation in the UBRC can have considerable impacts on regional water security and agricultural productivity. This study is a step toward assessing the potential impact on the water resources in a semi-arid catchment. This is a first-order analysis, yet important to understand the hydrological response of UBRC under the past, present, and future climate change scenarios. It can be used to develop sustainable water resource management to meet the future water demand for agriculture, domestic, industrial, and other purposes.

Acknowledgements We would like to acknowledge IISER Bhopal for providing institutional support. Amit Kumar Ph.D. is supported by IISER Bhopal.

Funding This research received no external funding.

Declarations

Conflict of interest The authors declare no conflict of interest.

Ethical approval This chapter does not contain any studies with human participants or animals performed by any of the authors.

Informed consent Not applicable.

References

- Aadhar, S., & Mishra, V. (2020). On the projected decline in droughts over south asia in cimp6 multimodel ensemble. *Journal of Geophysical Research: Atmospheres*, *125*(20), 1–18.
- Abbas, S., & Dastgeer, G. (2021). Analysing the impacts of climate variability on the yield of kharif rice over Punjab, Pakistan. In: *Natural Resources Forum*, Wiley Online Library, pp 1–21.
- Abbas, S., & Kousar, S. (2021). Spatial analysis of drought severity and magnitude using the standardized precipitation index and streamflow drought index over the upper indus basin, Pakistan. *Environment, Development and Sustainability*, *23*, 1–27.
- Abbas, S., Shirazi, S. A., Hussain, M. S., Yaseen, M., Shakarullah, K., Wahla, S. S., & Khurshid, M. (2020). *Impact of climate change on forest cover: Implications for carbon stock assessment and sustainable development in hkh region-Pakistan.*, *21*(1), 66–81.
- Abbas, S., Kousar, S., & Pervaiz, A. (2021). Effects of energy consumption and ecological footprint on co 2 emissions: An empirical evidence from Pakistan. *Environment, Development and Sustainability*, *23*, 1–18.
- Abbas, S., Kousar, S., Shirazi, S. A., Yaseen, M., & Latif, Y. (2021b). Illuminating empirical evidence of climate change: Impacts on rice production in the punjab regions, Pakistan. *Agricultural Research*, 1–16.
- Ahn, K. H., & Merwade, V. (2014). Quantifying the relative impact of climate and human activities on streamflow. *Journal of Hydrology*, *515*, 257–266.
- Anand, J., Gosain, A. K., & Khosa, R. (2018). Prediction of land use changes based on land change modeler and attribution of changes in the water balance of ganga basin to land use change using the swat model. *Science of the Total Environment*, *644*, 503–519.
- Arnold, J. G., Moriasi, D. N., Gassman, P. W., Abbaspour, K. C., White, M. J., Srinivasan, R., Santhi, C., Harmel, R., Van Griensven, A., Van Liew, M. W., et al. (2012). Swat: Model use, calibration, and validation. *Transactions of the ASABE*, *55*(4), 1491–1508.
- Asoka, A., Gleeson, T., Wada, Y., & Mishra, V. (2017). Relative contribution of monsoon precipitation and pumping to changes in groundwater storage in India. *Nature Geoscience*, *10*(2), 109–117.
- Babar, S., & Ramesh, H. (2015). Streamflow response to land use-land cover change over the nethravathi river basin, India. *Journal of Hydrologic Engineering*, *20*(10), 1–11.
- Chanapathi, T., & Thatikonda, S. (2020). Investigating the impact of climate and land-use land cover changes on hydrological predictions over the krishna river basin under present and future scenarios. *Science of The Total Environment*, *721*, 1–19.
- Chawla, I., & Mujumdar, P. (2015). Isolating the impacts of land use and climate change on streamflow. *Hydrology and Earth System Sciences*, *19*(8), 3633–3651.
- Desai, S., Singh, D., Islam, A., & Sarangi, A. (2020). Impact of climate change on the hydrology of a semi-arid river basin of India under hypothetical and projected climate change scenarios. *Journal of Water and Climate Change*, *12*, 969–996.
- Devi, R. M., Patasaraiya, M. K., Sinha, B., Bisaria, J., & Dimri, A. (2020). Analyzing precipitation and temperature trends of Kanha and Satpura tiger reserve, central India. *Theoretical and Applied Climatology*, *140*, 1–16.
- Dibaba, W. T., Demissie, T. A., & Miegel, K. (2020). Watershed hydrological response to combined land use/land cover and climate change in highland ethiopia: Finchaa catchment. *Water*, *12*(6), 1801.
- Dubey, S. K., Sharma, D., Babel, M. S., & Mundetia, N. (2020). Application of hydrological model for assessment of water security using multi-model ensemble of cordex-South Asia experiments in a semi-arid river basin of India. *Ecological Engineering*, *143*, 1–14.

- Eyring, V., Bony, S., Meehl, G. A., Senior, C. A., Stevens, B., Stouffer, R. J., & Taylor, K. E. (2016). Overview of the coupled model intercomparison project phase 6 (cmip6) experimental design and organization. *Geoscientific Model Development*, 9(5), 1937–1958.
- Eyring, V., Cox, P. M., Flato, G. M., Gleckler, P. J., Abramowitz, G., Caldwell, P., Collins, W. D., Gier, B. K., Hall, A. D., Hoffman, F. M., et al. (2019). Taking climate model evaluation to the next level. *Nature Climate Change*, 9(2), 102–110.
- Gosain, A., Rao, S., & Basuray, D. (2006). *Climate change impact assessment on hydrology of indian river basins*. *Current science* (pp. 346–353)
- Gupta, V., Singh, V., & Jain, M. K. (2020). Assessment of precipitation extremes in India during the 21st century under ssp1–1.9 mitigation scenarios of cmip6 gcms. *Journal of Hydrology*, 590, 1–16.
- Hayes, M. J., Svoboda, M. D., Wihite, D. A., & Vanyarkho, O. V. (1999). Monitoring the 1996 drought using the standardized precipitation index. *Bulletin of the American meteorological society*, 80(3), 429–438.
- Hengade, N., & Eldho, T. (2016). Assessment of lulc and climate change on the hydrology of ashti catchment, India using vic model. *Journal of Earth System Science*, 125(8), 1623–1634.
- Huang, J., Ji, M., Xie, Y., Wang, S., He, Y., & Ran, J. (2016). Global semi-arid climate change over last 60 years. *Climate Dynamics*, 46(3–4), 1131–1150.
- Kumar, A., Sarthi, P. P., Kumari, A., & Sinha, A. K. (2021). Observed characteristics of rainfall indices and outgoing longwave radiation over the Gangetic plain of India. *Pure and Applied Geophysics*, 178, 1–13.
- Kundu, S., Khare, D., & Mondal, A. (2017a). Individual and combined impacts of future climate and land use changes on the water balance. *Ecological Engineering*, 105, 42–57.
- Kundu, S., Khare, D., & Mondal, A. (2017b). Past, present and future land use changes and their impact on water balance. *Journal of environmental management*, 197, 582–596.
- Li, C., Zwiers, F., Zhang, X., Li, G., Sun, Y., & Wehner, M. (2020). Changes in annual extremes of daily temperature and precipitation in cmip6 models. *Journal of Climate*, 34, 1–61.
- Liu, C., & Xia, J. (2004). Water problems and hydrological research in the yellow river and the Huai and Hai river basins of China. *Hydrological Processes*, 18(12), 2197–2210.
- Luo, M., Liu, T., Meng, F., Duan, Y., Frankl, A., Bao, A., & De Maeyer, P. (2018). Comparing bias correction methods used in downscaling precipitation and temperature from regional climate models: A case study from the Kaidu river basin in Western China. *Water*, 10(8), 1046.
- Mann, H. B. (1945). *Nonparametric tests against trend*. *Econometrica: Journal of the econometric society* (pp. 245–259)
- Mendoza, P. A., Clark, M. P., Mizukami, N., Newman, A. J., Barlage, M., Gutmann, E. D., Rasmussen, R. M., Rajagopalan, B., Brekke, L. D., & Arnold, J. R. (2015). Effects of hydrologic model choice and calibration on the portrayal of climate change impacts. *Journal of Hydrometeorology*, 16(2), 762–780.
- Moriiasi, D. N., Arnold, J. G., Van Liew, M. W., Bingner, R. L., Harmel, R. D., & Veith, T. L. (2007). Model evaluation guidelines for systematic quantification of accuracy in watershed simulations. *Transactions of the ASABE*, 50(3), 885–900.
- Naik, N., Beg, Z., Kumar, A., & Gaurav, K. (2021). Groundwater dynamics in the betwa river catchment in central india. In: EGU General Assembly Conference Abstracts, pp EGU21–15373
- Narsimlu, B., Gosain, A. K., & Chahar, B. R. (2013). Assessment of future climate change impacts on water resources of upper Sind river basin, India using swat model. *Water resources management*, 27(10), 3647–3662.
- O’Neill, B. C., Tebaldi, C., Vuuren, D. P. V., Eyring, V., Friedlingstein, P., Hurtt, G., et al. (2016). The scenario model intercomparison project (scenariomip) for cmip6. *Geoscientific Model Development*, 9(9), 3461–3482.
- O’Neill, B. C., Kriegler, E., Riahi, K., Ebi, K. L., Hallegatte, S., Carter, T. R., et al. (2014). A new scenario framework for climate change research: The concept of shared socioeconomic pathways. *Climatic Change*, 122(3), 387–400.
- Palmate, S. S. (2017). Modelling spatiotemporal land dynamics for a trans-boundary river basin using integrated cellular automata and markov chain approach. *Applied geography*, 82, 11–23.
- Paul, S., Ghosh, S., Oglesby, R., Pathak, A., Chandrasekharan, A., & Ramsankaran, R. (2016). Weakening of Indian summer monsoon rainfall due to changes in land use land cover. *Scientific reports*, 6(1), 1–10.
- Rao, K. K., Patwardhan, S., Kulkarni, A., Kamala, K., Sabade, S., & Kumar, K. K. (2014). Projected changes in mean and extreme precipitation indices over India using precis. *Global and Planetary Change*, 113, 77–90.
- Reichle, R. H., & Koster, R. D. (2004). Bias reduction in short records of satellite soil moisture. *Geophysical Research Letters*, 31(19)
- Roxy, M. K., Ghosh, S., Pathak, A., Athulya, R., Mujumdar, M., Murtugudde, R., et al. (2017). A threefold rise in widespread extreme rain events over central India. *Nature Communications*, 8(1), 1–11.

- Saharwardi, M. S., Mahadeo, A. S., & Kumar, P. (2021). Understanding drought dynamics and variability over bundelkhand region. *Journal of Earth System Science*, 130(3), 1–16.
- Schwinning, S., Sala, O. E., Loik, M. E., & Ehleringer, J. R. (2004). Thresholds, memory, and seasonality: Understanding pulse dynamics in arid/semi-arid ecosystems. *Oecologia*, 141, 191–193.
- Shah, R., & Srivastava, R. (2019). Effect of climate change on cloud properties over Arabian sea and Central India. *Pure and Applied Geophysics*, 176(6), 2729–2738.
- Sharmila, S., Joseph, S., Sahai, A., Abhilash, S., & Chattopadhyay, R. (2015). Future projection of Indian summer monsoon variability under climate change scenario: An assessment from cmip5 climate models. *Global and Planetary Change*, 124, 62–78.
- Singh, A., Gaurav, K., Meena, G. K., & Kumar, S. (2020). Estimation of soil moisture applying modified dubois model to sentinel-1; A regional study from central India. *Remote Sensing*, 12(14), 2266.
- Sinha, R. K., Eldho, T., & Subimal, G. (2020). Assessing the impacts of land use/land cover and climate change on surface runoff of a humid tropical river basin in Western Ghats, India. *International Journal of River Basin Management*, 1–12.
- Swain, S. S., Mishra, A., Sahoo, B., & Chatterjee, C. (2020). Water scarcity-risk assessment in data-scarce river basins under decadal climate change using a hydrological modelling approach. *Journal of Hydrology*, 590, 125260.
- Tanksali, A., & Soraganvi, V. S. (2021). Assessment of impacts of land use/land cover changes upstream of a dam in a semi-arid watershed using qswat. *Modeling Earth Systems and Environment*, 7(4), 2391–2406.
- Taylor, K. E. (2001). Summarizing multiple aspects of model performance in a single diagram. *Journal of Geophysical Research: Atmospheres*, 106(D7), 7183–7192.
- Teutschbein, C., & Seibert, J. (2012). Bias correction of regional climate model simulations for hydrological climate-change impact studies: Review and evaluation of different methods. *Journal of hydrology*, 456, 12–29.
- Tsarouchi, G., & Buytaert, W. (2018). Land-use change may exacerbate climate change impacts on water resources in the Ganges basin. *Hydrology and Earth System Sciences*, 22(2), 1411–1435.
- Vu, M., Raghavan, S. V., & Liong, S. Y. (2012). Swat use of gridded observations for simulating runoff-a vietnam river basin study. *Hydrology and Earth System Sciences*, 16(8), 2801–2811.
- Wagner, P. D., Bhallamudi, S. M., Narasimhan, B., Kantakumar, L. N., Sudheer, K., Kumar, S., et al. (2016). Dynamic integration of land use changes in a hydrologic assessment of a rapidly developing Indian catchment. *Science of the Total Environment*, 539, 153–164.
- Wang, G., Zhang, Y., Liu, G., & Chen, L. (2006). Impact of land-use change on hydrological processes in the Maying river basin, China. *Science in China Series D: Earth Sciences*, 49(10), 1098–1110.
- Wang, M., Zhang, D. Q., Su, J., Dong, J. W., & Tan, S. K. (2018). Assessing hydrological effects and performance of low impact development practices based on future scenarios modeling. *Journal of Cleaner Production*, 179, 12–23.
- Yaseen, M., Waseem, M., Latif, Y., Azam, M. I., Ahmad, I., Abbas, S., et al. (2020). Statistical downscaling and hydrological modeling-based runoff simulation in trans-boundary Mangla watershed Pakistan. *Water*, 12(11), 1–21.
- Zhang, B., Shrestha, N. K., Daggupati, P., Rudra, R., Shukla, R., Kaur, B., & Hou, J. (2018). Quantifying the impacts of climate change on streamflow dynamics of two major rivers of the Northern lake Erie basin in Canada. *Sustainability*, 10(8), 2897.

Authors and Affiliations

Amit Kumar¹  · Abhilash Singh¹ · Kumar Gaurav¹

Abhilash Singh
sabilash@iiserb.ac.in

Kumar Gaurav
kgaurav@iiserb.ac.in

¹ Department of Earth and Environmental Sciences, Indian Institute of Science Education and Research Bhopal, Bhopal, India